# Part I

## An overview of deep learning and its applications in COVID-19 and tuberculosis

**IOP** Publishing

Multimodality Imaging, Volume 2
Heart, lungs and peripheral organs
**Mainak Biswas and Jasjit S Suri**

# Chapter 1

## An overview of AI applications in medical imaging for COVID-19-related brain and heart injuries

**Harshit Sharma, Radhakrishn Birla, Mainak Biswas and Jasjit S Suri**

Artificial intelligence (AI) has significantly impacted the field of medicine, especially radiology, in recent years. The COVID-19 pandemic has caused a devastating impact, with over 416 million people infected and more than 5.8 million lives lost as of February 23, 2022. Although there have been approximately 228,391 publications on COVID-19, only a few articles have focused on the influence of AI and medical imaging on infected patients with comorbidities.

A comprehensive study has recently been conducted to investigate the various pathways that lead to heart and brain damage in individuals who have contracted COVID-19. This study has provided valuable insights into the importance of medical imaging in the management of patients with comorbid conditions, utilizing statistical data on COVID-19 symptoms. Common symptoms associated with COVID-19 include hypoxia, arrhythmias, plaque rupture, coronary thrombosis, encephalitis, ischemia, inflammation, venous and lung injury, as well as thromboembolism. The research primarily focuses on the application of AI in identifying specific tissues in COVID-19 patients and assessing the severity of their illness through the analysis of medical images. Given the limited medical resources available to governments worldwide in the fight against the pandemic, the use of image-based AI has become increasingly essential for the detection and diagnosis of COVID-19.

The integration of imaging and AI-based tissue classification, along with preliminary test probability and COVID-19 symptoms, has revealed a promising method to evaluate the potential danger posed by patients with comorbidities. Techniques like these can play a crucial role in monitoring and enhancing the healthcare system during and after the epidemic. Keywords such as COVID-19, comorbidity, pathophysiology, heart, brain, lung, imaging, artificial intelligence, and risk assessment have been identified as important factors in this context.

doi:10.1088/978-0-7503-2352-9ch1

## 1.1 Introduction

In December 2019, a new coronavirus called 'severe acute respiratory distress syndrome coronavirus 2' (SARS-CoV-2) was identified in Wuhan, the capital of Hubei Province in the People's Republic of China [1]. Initially, the Chinese government referred to the illness caused by the viral infection as 'new coronavirus pneumonia' (NCP), while the World Health Organization (WHO) named it 'coronavirus disease 2019' (COVID-19). A global public health emergency was declared on January 30, 2020 [2]. The primary mode of transmission for SARS-CoV-2 is believed to be by means of respiratory droplets or nasal secretions [3]. Interhuman transmission was first observed by Jasper Fuk-Woo Chan *et al* during their investigation at the University of Hong Kong-Shenzhen Hospital [4]. As of July 16, 2022, the pandemic had spread to more than 200 countries, resulting in over 416 million infections and 5.8 million deaths due to its high contagion rate (Ro = 2.7) [5], as shown in figure 1.1.

Recent studies have revealed that individuals with preexisting conditions face a higher risk of severe consequences due to COVID-19 [6–10]. In a specific study focused on COVID-19 patients, diabetic individuals (48, 24.9%) exhibited significantly higher mortality rates (81.3% vs. 47.6%) and ICU hospitalization rates (66.7% vs. 41.4%) compared to non-diabetic individuals (145, 75.1%) [11]. Diabetic individuals also experienced severe inflammatory reactions and coagulopathy in the heart, liver, and kidneys. Infected individuals with chronic disorders such as diabetes, renal disease, dyslipidemia, hypertension, cardiovascular diseases, and chronic obstructive pulmonary disease (COPD) had a higher prevalence of heart and

**Figure 1.1.** COVID-19 is distributed over 213 countries on a world map (courtesy: John Hopkins University).

brain (H&B) damage [12–16]. SARS-CoV-2 has been found to infect the thin lining of the epithelial cells that line the arteries, leading to atherosclerosis and arterial inflammatory disease, which are significant contributors to cardiovascular diseases (CVDs) and H&B damage [12, 17–21]. This may be attributed to a decrease in the production of angiotensin-converting enzyme 2 (ACE2), which results in endothelial dysfunction and exacerbates existing atherosclerosis [22, 23]. When individuals with comorbidities undergo image screening, it has been observed that they exhibit a wide range of preliminary test probabilities (PTPs) for COVID-19, ranging from mild to severe [24]. Conventional cardiovascular risk factors (CCVRFs), such as imaging techniques of the heart or alternative indicators used as substitutes for assessing coronary artery disease (e.g., carotid artery disease), are closely associated with comorbid patients. COVID-19 severity prediction models can benefit from the incorporation of both biomarkers and imaging [25–30]. Figure 1.2 illustrates the connections between SARS-CoV-2 and comorbidities, as well as the survival rates of COVID-19 individuals with and without diabetes.

The expression of ACE2 can lead to scarring and potential artery rupture [31–34]. Therefore, it is essential to evaluate CCVRF alongside imaging in individuals with COVID-19 and other comorbidities [35]. In stage two of the disease, when patients are severely affected by COVID-19, there is a higher risk of heart damage or the release of troponin T (TnT). Imaging has proven to be valuable in keeping track of tissue scarring caused by COVID-19 [35–39].

Different imaging modalities such as magnetic resonance imaging (MRI), computed tomography (CT), and ultrasound can be employed to detect COVID-19 symptoms in patients [40–44]. These imaging techniques offer the advantage of visualizing the scar tissue caused by the disease. However, a drawback is their inability to provide a 'risk assessment' on their own. Artificial intelligence (AI) technologies have the potential to leverage information from imaging modalities and generate more precise predictions, enabling accurate identification of tissues and disease processes [45–51]. The combination of AI and medical imaging (MI) has demonstrated significant advancements in diagnosis, risk stratification, rapid patient

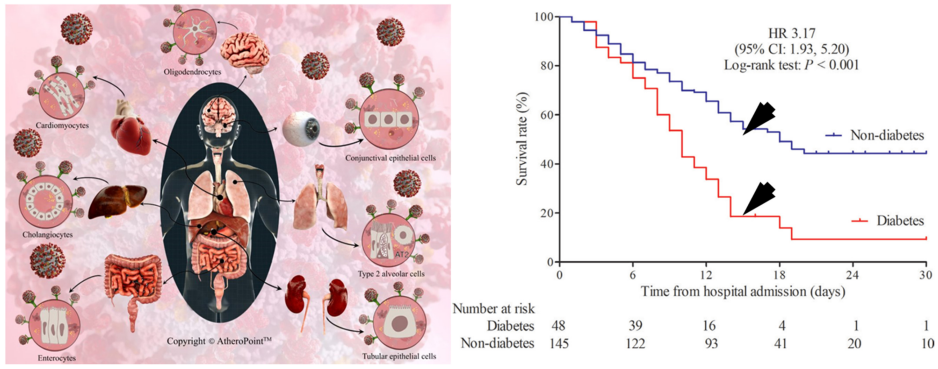


**Figure 1.2.** (a) SARS-CoV-2 and its link with other comorbidities, and (b) COVID-19 diabetes and non-diabetic patients' mortality rates compared (with permission to reprint [11]).

evaluation, disease monitoring, and early intervention [40, 48, 52–57]. Consequently, this review focuses on the utilization of AI-based tissue characterization through medical imaging in comorbid patients affected by COVID-19.

The chapter is organized as follows: section 1.2 examines the physiological mechanisms underlying the four pathways that result in heart and brain injuries. Section 1.3 presents an overview of the justification for utilizing imaging in the context of the COVID-19 pandemic. Section 1.4 provides an in-depth exploration of utilizing AI-based tissue characterization for risk assessment. Ultimately, the paper concludes with a thorough critical analysis.

## 1.2 SAR-CoV-2 pathophysiology in the context of heart and brain injury

Numerous studies indicate that SARS-CoV-2 relies on the ACE2 receptor for cell entry, achieved by binding to the spike protein (S protein) on the cell surface [58–60] (see figure 1.2). ACE1 and ACE2 are carboxypeptidase enzymes that are structurally similar but have distinct roles in the renin-angiotensin-aldosterone system (RAAS) [61]. The ACE2 is found in various cardiac cells, including, astrocytes (brain cells), enterocytes and type 2 pneumocytes [15, 61–63], and is recognized as a contributing factor to extrapulmonary complications. Figure 1.3 provides a comprehensive visual representation of how SARS-CoV-2 induces cardiac and brain damage through four

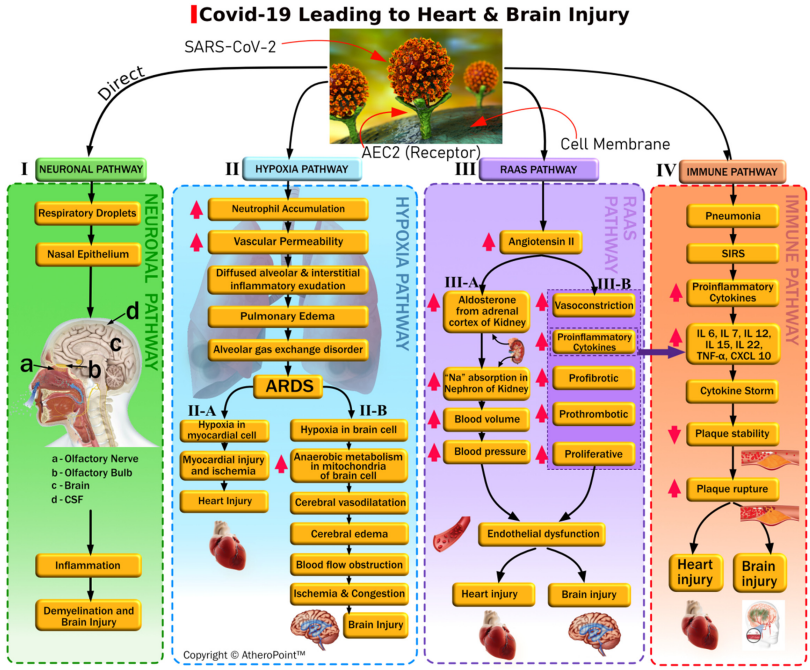


**Figure 1.3.** We have shown in four pathways how COVID-19 can cause brain and heart injury. Brain image in pathway I: http://debuglies.com/2020/01/23/olfactory-disturbances-have-implications-in-mental-and-emotional-well-being-health/ (courtesy of Debug Lies).

distinct paths: (i) the RAAS pathway, (ii) the immune pathway, (iii) the neural pathway, and (iv) the hypoxia pathway. These pathways will be further discussed, along with the resulting injuries, which may encompass infectious toxic encephalopathy, acute cerebrovascular diseases and viral encephalitis.

(i) The neural pathway (figure 1.3, the first pathway): Recent epidemiological investigations have highlighted genomic similarities between MERS, SARS-CoV-1, and SARS-CoV-2 [6, 64, 65]. Prior research has demonstrated that coronaviruses, including SARS-CoV-1, have the ability to enter the brain and directly infect it [66, 67]. In figure 1.3, the sagittal brain image representing the neural pathway illustrates the olfactory nerve and bulb, labeled as 'a' and 'b,' respectively [68–70]. It has been observed that individuals infected with SARS-CoV-2 may experience symptoms such as dysgeusia (taste loss) and anosmia (loss of smell) [64, 71–73]. Furthermore, a mouse experiment where the olfactory bulb was surgically removed demonstrated a limitation of CoV within the central nervous system (CNS) [74]. These findings suggest that the neural pathway could be one of the potential routes for SARS-CoV-2.

(ii) The hypoxia pathway (figure 1.3, the second pathway): Following the entry of the coronavirus into lung parenchyma cells, there is a reduction in ACE2 levels, leading to the accumulation of neutrophils, increased vascular permeability, and the release of diffuse alveolar and interstitial exudates. This process contributes to the development of acute respiratory distress syndrome (ARDS) and pulmonary edema [75]. ARDS is described by significant irregularities in the composition of blood gases, causing an imbalance of oxygen and carbon dioxide and leading to decreased blood oxygen levels [76, 77]. Prolonged hypoxia can induce myocardial ischemia and cardiac damage [78, 79] (see figure 1.3, pathway II-A). In the brain, hypoxia is the primary cause of cerebral vasodilation, edema, and reduced blood flow due to increased anaerobic metabolism in brain cell mitochondria. This can lead to cerebral ischemia and acute cerebrovascular disorders, such as acute ischemic stroke [71, 80] (see figure 1.3, pathway II-B).

(iii) The RAAS pathway (figure 1.3, the third pathway): The renin-angiotensin-aldosterone system (RAAS) pathway plays a critical role in regulating blood pressure and electrolyte balance. Disruption of this pathway can contribute to the development of cardiovascular disorders [15]. Prior to SARS-CoV-2 invasion, angiotensin I (Ang I) is converted to angiotensin II (Ang II) by ACE1. Ang II causes vasoconstriction and possesses pro-inflammatory, prothrombotic, and proliferative properties that can negatively impact the hemostasis and vascular tone [77, 80]. Conversely, ACE2 counteracts the effects of Ang II by converting it to Ang (1–7), which has mitigating effects [75, 78]. Both ACE2 and Ang (1–7) have protective effects on the cardiovascular and cerebrovascular systems [61]. SARS-CoV-2 infection disrupts the RAAS, leading to injuries in the heart and brain through two distinct pathways. The primary mechanism involves an

increase in Ang II levels due to a decrease in ACE2 levels (figure 1.3, pathway III-A). Firstly, elevated Ang II levels stimulate the adrenal cortex in the kidney, resulting in increased aldosterone production. Aldosterone, a steroid hormone, facilitates the reabsorption of sodium and water in the distal tubule and collecting duct of the nephron [81]. This leads to an increase in blood volume and raises blood pressure, causing endothelial dysfunction and subsequent damage to the heart and brain [82]. Secondly, elevated Ang II levels and decreased ACE2 levels contribute to endothelial dysfunction in arterial walls, which can be observed in arterial wall images [21] (see figure 1.3, pathway III-B). High levels of Ang II can also trigger the release of pro-inflammatory cytokines, contributing to a cytokine storm.

(iv) The immune pathway (figure 1.3, the fourth pathway): In recent studies, SARS-CoV-2 viral pneumonia has been linked to an elevated inflammatory response known as a 'cytokine storm' [7, 77, 83, 84]. Advanced stages of severe COVID-19 are characterized by increased levels of inflammatory cytokines, which can contribute to multiple organ failure [85–87]. Inflammatory markers such as IL-6, IL-7, IL-12, IL-15, IL-22, TNF-α, and CXCL-10 have been associated with plaque destabilization. This increased inflammation can potentially lead to plaque rupture and subsequent damage to the heart and brain [37, 68–70, 80, 85–87, 89–91].

## 1.3 The role of imaging in patients with comorbidities and COVID-19

COVID-19 leads to significant damage to the heart and brain through four pathways (neuronal, hypoxia, RAAS, and immunological), as discussed earlier. This highlights the need for increased utilization of medical imaging (MI) to expedite assessments, differential diagnoses, and patient management [92] with appropriate safety measures. The choice of imaging modality depends on symptom severity, with consideration for portability and invasiveness. Portable and non-invasive ultrasound imaging in B-Mode is suitable for low-risk individuals, while x-rays, magnetic resonance imaging (MRI), and computed tomography (CT) are non-portable and can be used for patients with a medium risk level [40, 41]. Invasive imaging techniques like intravascular ultrasonography (IVUS) and ventriculography are reserved for life-threatening situations [42, 43, 98–100]. Ultrasound is particularly advantageous due to its rapidity, reproducibility, cost-effectiveness, radiation-free nature, and portability. It can be performed in isolation, minimizing the risk of COVID-19 transmission [101, 102].

Throughout the early and later stages of the pandemic, various imaging modalities have proven effective. X-ray imaging of the lungs has revealed different patterns, signaling the advancement of COVID-19 at different stages and aiding in treatment planning [103]. Chest CT scans have shown lung involvement in nearly 86% of COVID-19 patients, affecting at least one lobe [104]. Chest MRI scans have revealed pulmonary tissue consolidation, diffusion-restricted areas, and lung injury

in COVID-19 patients [105]. MRI examinations of recovered patients have identified myocardial edema and late gadolinium augmentation, indicating long-term cardiac damage requiring ongoing care even after recovery [106]. MR scans of COVID-19 patients have demonstrated myocardial inflammation, highlighting cardiac damage caused by the cytokine storm associated with the infection (Pathway IV) [107]. Studies have also investigated the impact of COVID-19 on the brain, with MRI images showing hemorrhagic rim enhancing lesions in specific brain regions [108] (figure 1.4). Abnormal findings have been observed in brain MRI scans of COVID-19 patients, and combined CT and ultrasound investigations have revealed liver disease and gallbladder abnormalities [109, 110]. Recent MRI scans of COVID-19 patients' olfactory bulbs have revealed inflammatory occlusion caused by the interaction between SARS-CoV-2 and the ACE2 protein expressed in the olfactory epithelium, resulting in the loss of olfactory function [111].

Invasive imaging techniques are employed to ascertain the diagnosis of individuals with COVID-19 with significant comorbidities. One trial utilized intravascular ultrasonography (IVUS) in combination with stenting for a COVID-19 patient who experienced a myocardial infarction [112] (figure 1.5). Precautions regarding invasive imaging techniques are further explained in section 1.5. Another study employed ventriculography to detect takotsubo syndrome, a type of cardiac damage associated with COVID-19 [113]. In several trials, MI of COVID-19 patients played a critical role in assessing tissue damage and determining the severity of infection, even in the absence of obvious signs [39, 114]. Therefore, MI is recommended for evaluating the degree of damage to cardiac and cerebral tissues in individuals with

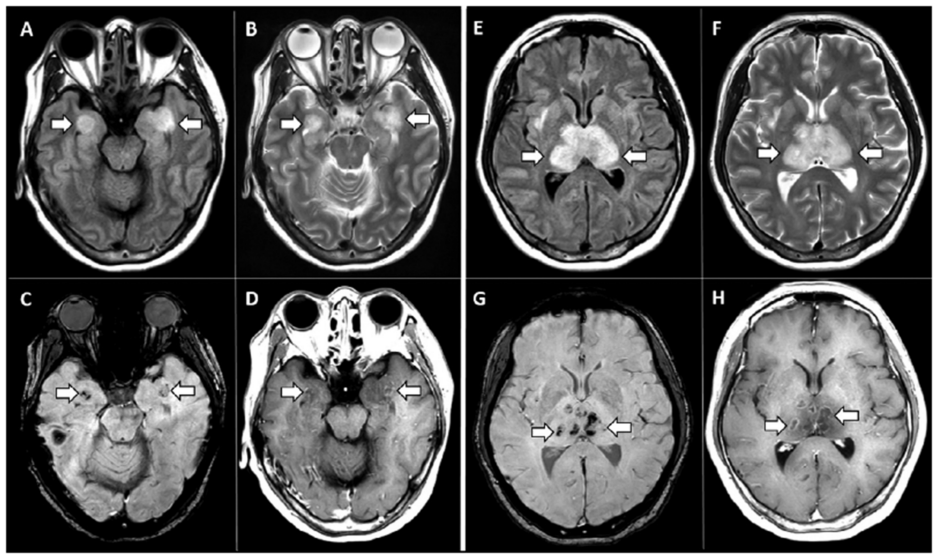


**Figure 1.4.** The MRI scan of a patient with COVID-19 showed evidence of bleeding. T2 FLAIR hyperintensity was observed in the paired medial temporal lobes and thalami (A, B, E, F), and the hemorrhage was identified by a hypointense signal intensity on susceptibility-weighted images (C, G). Additionally, postcontrast imaging revealed rim enhancement (D, H) (reprinted with permission [108]).

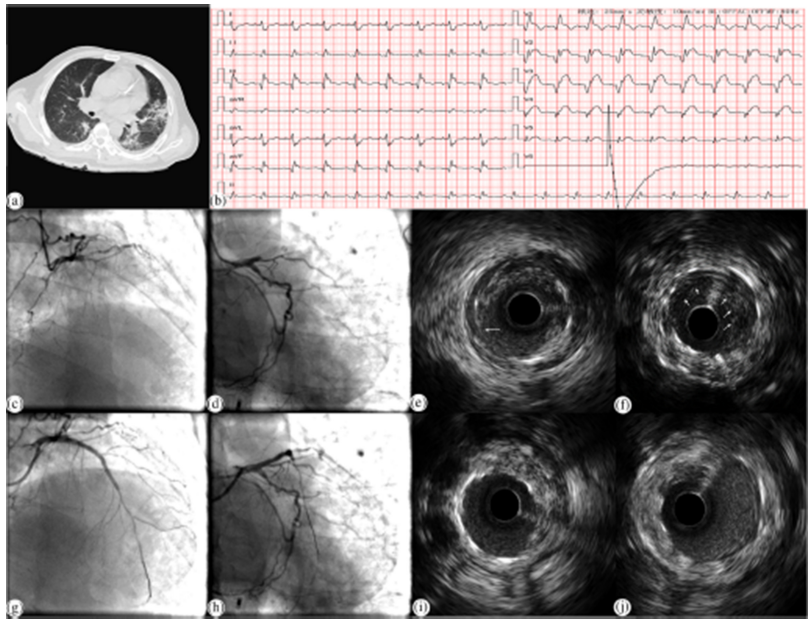

**Figure 1.5.** In a COVID-19 patient with myocardial infarction, both chest CT and intravascular ultrasound (IVUS) were utilized for diagnostic purposes. The findings from these imaging techniques are as follows: (a) Chest CT scan revealed localized fibrinous exudative alterations, which are associated with viral pneumonia. (b) ECG data showed ST-segment elevations in leads V1–V5 when the patient experienced chest pain. (c, d) Coronary angiography (CAG) indicated occlusion in the proximal segment of the left anterior descending artery (LAD). (e, f) Blood flow in the LAD was restored after the placement of two drug-eluting stents (DESs). (g) IVUS revealed a dissection distal to the stent in the LAD, specifically from the 7–12 o'clock position. (h) A low echogenic shadow with dispersed increased echogenic flicker was observed, indicating the presence of a thrombus. (i) The dissection was no longer visible after the DES was implanted and the stent was adequately inflated. (j) The thrombus disappeared following the intervention. These findings were obtained from a published study and are reprinted with permission [112].

COVID-19 throughout their lifetime. Individuals with preexisting medical conditions who have contracted COVID-19 are particularly vulnerable and should undergo MI examination from the time of diagnosis. MI can also be beneficial for COVID-19 patients with deep vein thrombosis (DVT). An analysis found that patients suffering from COVID-19 and DVT had a worse prognosis compared to those lacking DVT. The DVT group had a higher rate of ICU admission (18.2%), lower rate of discharge (48.5%), and higher mortality rate (38.5%) [115].

However, the evaluation, diagnosis, and monitoring processes for myocardial infarction imaging can be challenging due to the exponential nature of the pandemic, limited medical resources, and a shortage of radiologists. These factors contribute to time-consuming processes and a higher risk of errors [116–118]. To address these challenges, the utilization of artificial intelligence (AI) in medical imaging (MI) for tissue characterization can offer valuable support. AI-based systems have the potential to be scaled up to meet the demands of the pandemic,

facilitating rapid MI assessments and diagnoses during the COVID-19 outbreak [119–121].

Based on the severity of symptoms and patient presentation, AI-driven assessments have the capability to classify or categorize the risk level into different categories, including zero-risk, low, low-medium, high-medium, low-high, or high-high risk [120, 122], as illustrated in figure 1.6. The choice of imaging modality depends on the assessed risk level. For zero-risk patients, no imaging is necessary.

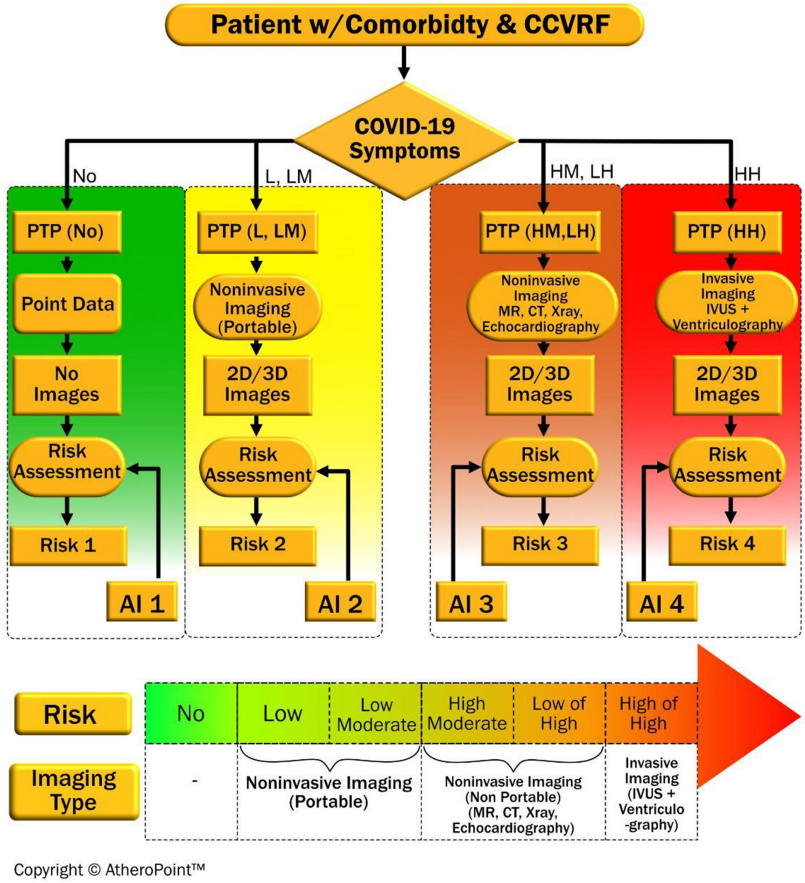


**Figure 1.6.** AI-based risk assessment plays a crucial role in managing comorbidity patients with COVID-19, offering valuable insights and aiding in healthcare administration [54, 55, 127–129]. The implementation of AI in healthcare encompasses various systems that enable accurate decision-making in patient monitoring, diagnosis, management, and treatment. In the field of medical imaging, artificial intelligence has gained significant importance due to the abundant volume of three-dimensional data accessible and the necessity to characterize and quantify diseases utilizing imaging observations [130–132]. Tissue imaging and classification are particularly vital as they directly impact decisions regarding the severity of COVID-19 in patients [133–135]. The key advantage of AI technologies lies in their ability to be trained to emulate the cognitive actions of physicians, allowing for the prediction of disease severity in asymptomatic patients. Several machine learning (ML)-based approaches have effectively utilized AI to combat COVID-19 within a short timeframe [136, 137].

Portable imaging modalities are suitable for patients at zero-risk and low-medium risk levels. Non-portable imaging techniques such as MRI, CT, x-ray, and echocardiography are appropriate for high-medium and low-high risk patients. Invasive imaging methods like IVUS and ventriculography are reserved for high-high risk patients. Precise evaluation of diagnostic results and patient categorization into specific risk groups can be achieved through pre-test probability (PTP) assessment [123–126]. Non-imaging biomarkers can be utilized by AI-based algorithms for risk assessment in zero-risk patients. Patients with low risk may undergo portable 2D/3D imaging modalities, such as ultrasound, while non-portable and invasive 2D/3D imaging modalities are suitable for low-medium risk patients. High-high risk patients may require invasive imaging techniques like ventriculography and IVUS. AI-driven MI plays a crucial role in assessing the risk level based on data obtained from multiple 2D/3D scans, and treatment decisions can be made accordingly. The subsequent section will focus on deep learning (DL)-based MI, particularly in the context of ultrasound scans for COVID-19 patients.

## 1.4 Machine learning and deep learning for tissue classification

The exponential rise in the number of patients during the pandemic and the limited availability of trained radiologists have presented challenges in achieving timely diagnoses. Nonetheless, the integration of AI and related technologies in healthcare holds significant promise in significantly reducing diagnosis times [119].

### 1.4.1 ML and DL architectures

The machine learning process consists of two stages. In stage I, various attributes from the images of COVID lesions are extracted and processed by a machine learning (ML) model to produce offline parameters. These parameters are then modified by test lesion photos, leading to intelligent categorization or inference. Figure 1.7 illustrates a typical machine learning system used for predicting risk class. The development of a CUSIP (image-based phenotype) relies on the event equivalent gold standard (EEGS) model [57, 138, 139]. Deep learning (DL) functions similarly to the visual cortex, employing multiple neural layers directly applied to tissue images for feature extraction and classification purposes [54]. Convolutional neural networks (CNN) [140], as shown in figure 1.8, are a common type of deep learning network used for medical image classification. Convolution and max-pooling operations are employed to extract features and carry out characterizations. Both ML and DL utilize a supervised learning method is employed, in which models are trained using preexisting data.

The previous sections have discussed how COVID-19 spreads through four distinct pathways and can cause damage to the heart and blood vessels (H&B). Myocardial infarction (MI) can be used to assess the level of tissue damage in these pathways, aiding healthcare professionals in developing appropriate treatment strategies for patients. The use of AI models for tissue classification based on medical images has been widely employed, both during the pandemic and in routine healthcare settings. In the subsequent sections, we will present a proposed approach

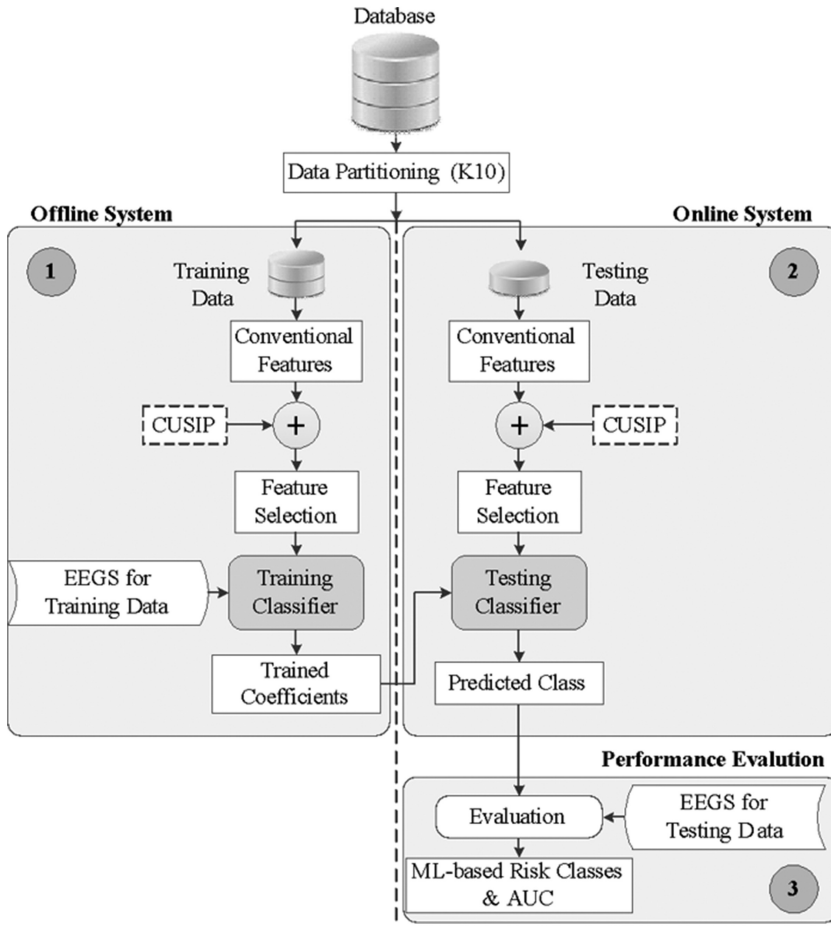


**Figure 1.7.** Classic ML model utilizing EEGS model.

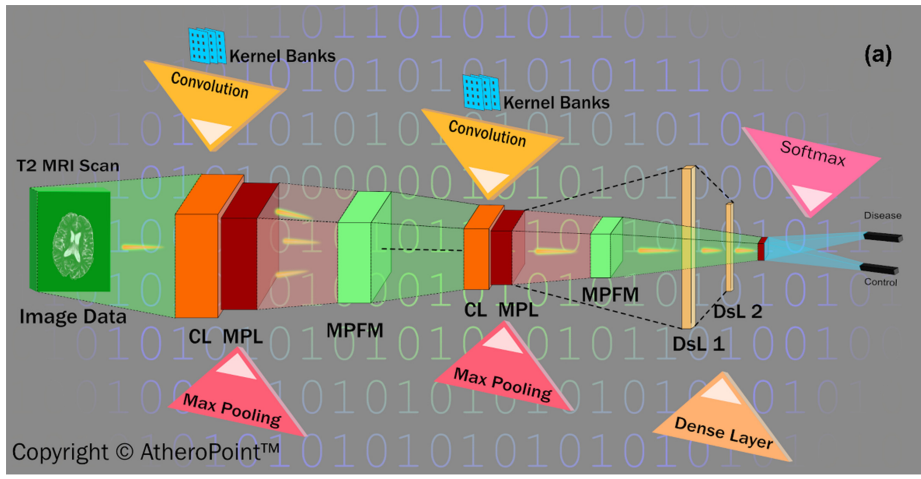


**Figure 1.8.** A convolution neural network (courtesy of AtheroPoint™, CA, USA).

for describing tissue classification using deep learning (DL) and provide specific examples of AI applications for each organ.

### 1.4.2 Tissue characterization ML system for stroke risk stratification

There are two primary types of AI-based approaches: (i) ML-based and (ii) DL-based methods [63, 141, 142]. ML-based techniques have been developed for the classification of symptomatic and asymptomatic plaques using ultrasound images. For instance, support vector machines (SVM), an ML-based method, were utilized to classify 346 carotid images into symptomatic and asymptomatic plaques [143, 144]. SVM classifiers create a hyperplane with the largest margin between points of two classes, known as support vectors. In the feature extraction step, texture analysis is employed to extract features such as entropy, symmetry, standard deviation, and run percentage [145, 146]. These features were then used to characterize plaque tissue lesions using SVM with a radial basis function (RBF) kernel, achieving an accuracy of 82.4%. Higher-order spectra (HOS) analysis has also been found to be significant in tissue characterization [130]. Another study combined HOS, discrete wavelet transformations (DWTs), and texture data from 146 patient images to create an SVM-RBF-based classifier [46, 130, 146–148]. This classifier achieved an accuracy of 91.7%. Additionally, DWT-based features were used with second-order kernels to differentiate tissues, resulting in an accuracy of 83.7%. To compare and evaluate various classifiers, a total of 346 scans from two distinct carotid plaque datasets (Portugal and the United Kingdom) were utilized. Various classifiers, including fuzzy classifier [154], k-nearest neighbor [152], radial basis probabilistic neural network [150], decision tree [151], Gaussian mixture model [149], naive Bayes classifier [153], and SVM [45] fuzzy classifier [154], were evaluated. The primary features employed encompassed trace transform [155], fuzzy gray level co-occurrence matrix [156], and fuzzy run-length matrix [157]. In the Portugal cohort, the fuzzy classifier attained the highest accuracy of 93.1%, while both the NBC and SVM-RBF kernels exhibited comparable performance at 85.3%. These AI models for plaque classification have been applied in various approaches for cardiovascular disease (CVD) risk stratification [27, 28, 158].

### 1.4.3 Vessel characterization, measurement, and risk stratification using ML/DL

#### *1.4.3.1 Chest CT and liver disease classification using AI*

During the COVID-19 pandemic, ML and DL techniques have been utilized for the classification of lung CT images, demonstrating varying degrees of effectiveness [159–164]. Kang *et al* achieved an accuracy of 95.5% by employing the utilization of representation learning to characterize chest CT scans without infection of data from COVID-19 patients [168]. Wang *et al* developed a DL-based system to differentiate CT scans of COVID-19 patients from those of non-infected individuals, yielding a receiver operating characteristic (ROC) curve with an area under the curve (AUC) of 0.959 [169].

Additionally, DL-based radiomics using shear wave elastography has been applied to distinguish diseased (fatty liver) ultrasound images and assess liver

fibrosis stages with an impressive accuracy of 100% [170–172]. This technique proves valuable for the identification and categorization of COVID-19 patients.

#### *1.4.3.2 Tissue characterization and risk stratification using artificial intelligence in lung CT*

Over the past few decades, numerous studies have been conducted ML and DL algorithms for the classification of lung CT images. These studies can be categorized into two types based on the number of risk stratification classes involved. The initial set of research focused on distinguishing COVID-19 pneumonia patients from non-COVID-19 pneumonia patients, resulting in a two-class scenario. The subsequent collection of studies explored multi-class paradigms.

In one study, the DenseNet 121 model was employed to create and segment lung masks, achieving an area under the curve (AUC) of 0.9, a sensitivity of 78.93%, and a specificity of 89.93% for categorizing COVID-19 and control patients [173]. Zhang *et al* adopted a three-class classification system that encompassed lung segmentation and categorization, including COVID-19, community pneumonia, and normal cases. They utilized the DeepLabv3 model for lung segmentation and 3D ResNet-18 for classification, achieving an accuracy of 92.49% and an AUC of 0.98 [174].

Other researchers also incorporated AI techniques in their CT lung scan studies. For instance, Li *et al* developed a DL system for CT lung analysis capable of predicting COVID-19 severity and progression [175]. Chen *et al* devised a UNet++ architecture to segment COVID-19-infected lung regions in CT scans [176, 177]. In a similar manner, Yang *et al* conducted lung segmentation on CT images by identifying pulmonary parenchyma and employing DenseNet for classification. Their approach achieved an accuracy of 92% and an AUC of 0.98 [178]. In another study, Oh *et al* employed x-ray chest images for both classification and segmentation, achieving an accuracy of 88.9% by employing a patch-based technique with the same network [179].

#### *1.4.3.3 AI-based plaque tissue characterization and risk stratification for cardiac health*

A DL-based platform is proposed for the treatment of COVID-19 patients with comorbidities. The platform utilizes preexisting facts obtained by patients suffering from COVID-19 worldwide to train the DL system. This data includes multiple ultrasound scans by patients suffering from COVID-19 with comorbidities who underwent treatment according to strict guidelines [93–97]. The AtheroEdgeTM system, which is capable of distinguishing and fragmenting plaque regions, automatically extracts tissue regions of interest (ROIs) from the ultrasound scans. The same AtheroEdgeTM technique is applied to extract ROIs from online patients' ultrasound scans. The DL model is then used to estimate the susceptibility of plaque in the online data, which is collected from testing patients after being trained with the offline data. The predictions obtained from this process are utilized to evaluate and support the clinical feasibility of the DL system.

## 1.5 Summary

In this review, we conducted an analysis of various imaging investigations performed on COVID-19 patients to assess the impact of the infection on key organs such as the lungs [104, 105], heart [106, 107], brain [108, 109] and liver. These imaging investigations were crucial in guiding the medical team in providing appropriate treatment for COVID-19 patients with varying degrees of symptoms. Among the available imaging modalities, ultrasonography was found to be particularly advantageous due to its portability and the ability to perform scans in isolation rooms, minimizing the risk of infection transmission across different wards. Similar mobility recommendations were also given for MRI and CT scanning as a preventive measure to curb the transmission of infections [180–182]. The availability of mass scanning for admitting patients would enable healthcare professionals to promptly design treatment plans and potentially save lives. In serious cases of patients suffering from COVID-19, the use of IVUS [98] and ventriculography (with necessary preventive measures) is recommended [42, 43, 99, 100] (figure 1.9).

The exponential growth of the COVID-19 pandemic presents challenges in evaluating and analyzing medical images in light of resource constraints and a shortage of radiologists. To address this, AI-driven medical imaging (MI) can be utilized to assist in the analysis, diagnosis, and risk stratification of patients suffering from COVID-19. AI systems have the capability to process large volumes of images simultaneously, enabling mass diagnosis to keep up with the rapidly evolving pandemic curve.

There are two main types of AI: ML and DL [54]. ML models use feature mining algorithms to make predictions, while DL models directly extract features from medical images, resulting in clearer images. An AI-based imaging-based risk evaluation model is recommended, where patients are categorized into risk levels such as zero/no-risk, low-risk, low-medium, medium-high, low-high, or high-high based on pre-test probability (PTP) tests [120, 122–126]. MI is then performed based on the patient's risk level, followed by AI utilization to assess the risk in MI. DL-driven tissue characterization systems can be particularly useful for ultrasound examinations and other imaging modalities. These DL-driven systems are trained using training data and evaluated using test data, allowing for the evaluation of tissue damage caused by COVID-19 infection.

Telemedicine, combined with AI support, can play a significant role in monitoring the well-being of patients. Telemedicine enables the management of infections by monitoring patients' health through Internet of Things (IoT) devices [183]. Social media platforms can also contribute to tracking patients' health and sharing important research findings through the application of big data analytics [184–186].

### 1.5.1 A note on COVID-19 precautions

In order to prevent infection, medical personnel must strictly adhere to guidelines [187–189]. This includes wearing eye protection, disposable gowns that are water-resistant, and disposable gloves, among other necessary precautions. Portable equipment should be used to avoid the need for relocating patients. Any

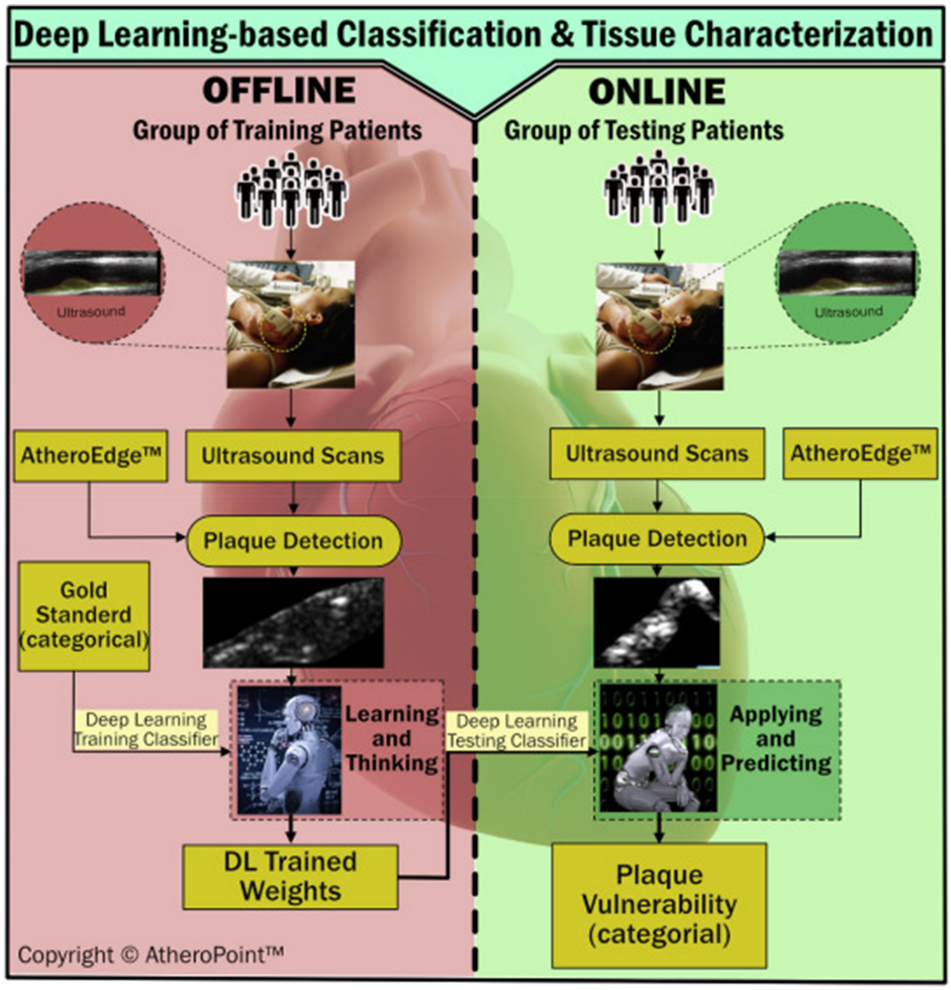


**Figure 1.9.** Proposed DL-based method for tissue characterization and classification of COVID-19 severity for patients with comorbidities (courtesy of AtheroPoint™, CA, USA).

medical imaging equipment that requires physical contact should be sterilized after each use, as shown in figure 1.10. Imaging equipment can be positioned outside the isolation room, allowing image acquisition through the window of the room to minimize direct interaction, as depicted in figure 1.10(b). When it is necessary to handle devices, a sterile protective disposable cover, such as an ultrasound probe cover as illustrated in figure 1.10(c), should be used.

## 1.6 Conclusion

COVID-19 can cause harm to the heart and blood vessels through four pathways: RAAS, neuronal, hypoxia, and immune. The severity of a patient's symptoms determines the level of risk associated with their condition, which in turn determines

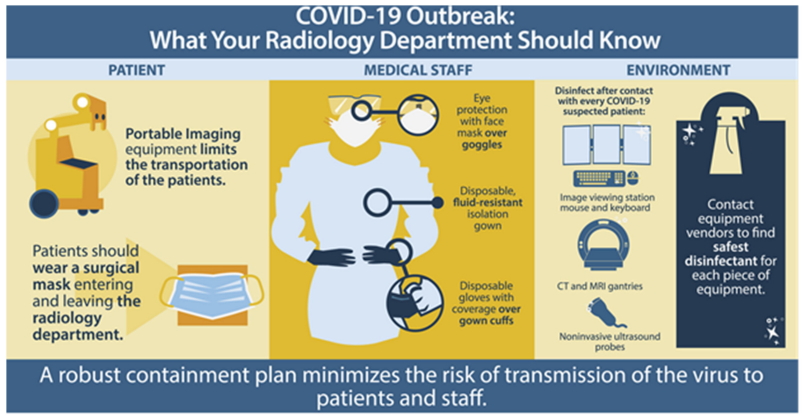


(a)


(b)


(c)

**Figure 1.10.** (a) Before taking scans, clinical personnel should follow these protection measures (with permission to reprint [187]); (b) Images shot through a window (with permission to reprint [188]); (c) probe covered with disposable sterile sheath (with permission to reprint [189]).

the type of imaging modality that should be used. Portable or non-portable invasive imaging modalities are recommended depending on the risk level, and appropriate safety measures must be taken during the imaging process. However, the limited availability of qualified radiologists poses a challenge to the widespread use of MI for COVID-19 diagnosis and evaluation.

To address this challenge, AI approaches such as ML and DL can be employed to expedite MI-based clinical evaluation and diagnosis. These AI methodologies have the potential to improve the efficiency and speed of diagnosing COVID-19 and assessing the risk associated with the disease. In particular, a DL-based system has been developed for COVID-19 diagnosis and risk classification, which can aid in

providing timely and accurate evaluations for individuals with comorbidities who are at a higher risk of experiencing severe health complications [190].

## References


[1] Yuen K-S, Ye Z-W, Fung S-Y, Chan C-P and Jin D-Y 2020 SARS-CoV-2 and COVID-19: the most important research questions *Cell Biosci.* **10** 1–5

[2] Coronavirus (COVID-19) outbreak (https://who.int/westernpacific/emergencies/covid-19)

[3] Coronavirus (https://who.int/health-topics/coronavirus#tab=tab_1)

[4] Chan J F-W, Yuan S, Kok K-H, To K K-W, Chu H, Yang J, Xing F, Liu J, Yip C C-Y and Poon R W-S 2020 A familial cluster of pneumonia associated with the 2019 novel coronavirus indicating person-to-person transmission: a study of a family cluster *Lancet* **395** 514–23

[5] Coronavirus (https://worldometers.info/coronavirus/)

[6] Wang D, Hu B, Hu C, Zhu F, Liu X, Zhang J, Wang B, Xiang H, Cheng Z and Xiong Y 2020 Clinical characteristics of 138 hospitalized patients with 2019 novel coronavirus–infected pneumonia in Wuhan, China *JAMA* **323** 1061–9

[7] Huang C, Wang Y, Li X, Ren L, Zhao J, Hu Y, Zhang L, Fan G, Xu J and Gu X 2020 Clinical features of patients infected with 2019 novel coronavirus in Wuhan, China *Lancet* **395** 497–506

[8] Shi S, Qin M, Shen B, Cai Y, Liu T, Yang F, Gong W, Liu X, Liang J and Zhao Q 2020 Association of cardiac injury with mortality in hospitalized patients with COVID-19 in Wuhan, China *JAMA Cardiol.* **5** 802–10

[9] Zhou F, Yu T, Du R, Fan G, Liu Y, Liu Z, Xiang J, Wang Y, Song B and Gu X 2020 Clinical course and risk factors for mortality of adult inpatients with COVID-19 in Wuhan, China: a retrospective cohort study *Lancet* **395** 1054–62

[10] Gao F, Zheng K I, Wang X B, Yan H D, Sun Q F, Pan K H, Wang T Y, Chen Y P, George J and Zheng M H 2020 Metabolic associated fatty liver disease increases COVID-19 disease severity in non-diabetic patients *J. Gastroenterol. Hepatol* **36** 204–7

[11] Yan Y, Yang Y, Wang F, Ren H, Zhang S, Shi X, Yu X and Dong K 2020 Clinical characteristics and outcomes of patients with severe covid-19 with diabetes *BMJ Open Diabetes Res. Care* **8** e001343

[12] Virani S S, Alonso A, Benjamin E J, Bittencourt M S, Callaway C W, Carson A P, Chamberlain A M, Chang A R, Cheng S and Delling F N 2020 Heart disease and stroke statistics—2020 update: a report from the American heart association *Circulation* **141** E139–596

[13] Zheng Y-Y, Ma Y-T, Zhang J-Y and Xie X 2020 COVID-19 and the cardiovascular system *Nat. Rev. Cardiol.* **17** 259–60

[14] Chen L, Li X, Chen M, Feng Y and Xiong C 2020 The ACE2 expression in human heart indicates new potential mechanism of heart injury among patients infected with SARS-CoV-2 *Cardiovasc. Res.* **116** 1097–100

[15] Williams V R and Scholey J W 2018 Angiotensin-converting enzyme 2 and renal disease *Curr. Opi. Nephrol. Hypertens.* **27** 35–41

[16] Wang B, Li R, Lu Z and Huang Y 2020 Does comorbidity increase the risk of patients with COVID-19: evidence from meta-analysis *Aging (Albany NY)* **12** 6049

[17] Cheng H, Wang Y and Wang G Q 2020 Organ-protective effect of angiotensin-converting enzyme 2 and its effect on the prognosis of COVID-19 *J. Med. Virol* **92** 726–30

[18] Libby P 2020 The heart in COVID19: primary target or secondary bystander? *JACC: Basic Transl. Sci.* **5** 537–42
[19] Clerkin K J, Fried J A, Raikhelkar J, Sayer G, Griffin J M, Masoumi A, Jain S S, Burkhoff D, Kumaraiah D and Rabbani L 2020 Coronavirus disease 2019 (COVID-19) and cardiovascular disease *Circulation* **141** 1648–55
[20] Libby P, Ridker P M and Maseri A 2002 Inflammation and atherosclerosis *Circulation* **105** 1135–43
[21] Suri J S, Kathuria C and Molinari F 2010 *Atherosclerosis Disease Management* (New York: Springer Science & Business Media)
[22] South A M, Diz D I and Chappell M C 2020 COVID-19, ACE2, and the cardiovascular consequences *Am. J. Physiol-Heart Circ. Physiol.* **318** H1084–90
[23] Dong B, Zhang C, Feng J B, Zhao Y X, Li S Y, Yang Y P, Dong Q L, Deng B P, Zhu L and Yu Q T 2008 Overexpression of ACE2 enhances plaque stability in a rabbit model of atherosclerosis *Arter. Thromb. Vasc. Biol.* **28** 1270–6
[24] Mossa-Basha M, Meltzer C C, Kim D C, Tuite M J, Kolli K P and Tan B S 2020 Radiology department preparedness for COVID-19: radiology scientific expert panel *Radiology* **296** 200988
[25] Kotsis V, Jamthikar A D, Araki T, Gupta D, Laird J R, Giannopoulos A A, Saba L, Suri H S, Mavrogeni S and Kitas G D 2018 Echolucency-based phenotype in carotid atherosclerosis disease for risk stratification of diabetes patients *Diabetes Res. Clin. Pract.* **143** 322–31
[26] Khanna N N, Jamthikar A D, Gupta D, Araki T, Piga M, Saba L, Carcassi C, Nicolaides A, Laird J R and Suri H S 2019 Effect of carotid image-based phenotypes on cardiovascular risk calculator: AECRS1. 0 *Med. Biol. Eng. Comput.* **57** 1553–66
[27] Khanna N N, Jamthikar A D, Araki T, Gupta D, Piga M, Saba L, Carcassi C, Nicolaides A, Laird J R and Suri H S 2019 Nonlinear model for the carotid artery disease 10-year risk prediction by fusing conventional cardiovascular factors to carotid ultrasound image phenotypes: a japanese diabetes cohort study *Echocardiography* **36** 345–61
[28] Cuadrado-Godia E, Jamthikar A D, Gupta D, Khanna N N, Araki T, Maniruzzaman M, Saba L, Nicolaides A, Sharma A and Omerzu T 2019 Ranking of stroke and cardiovascular risk factors for an optimal risk calculator design: logistic regression approach *Comput. Biol. Med.* **108** 182–95
[29] Khanna N N, Jamthikar A D, Gupta D, Piga M, Saba L, Carcassi C, Giannopoulos A A, Nicolaides A, Laird J R and Suri H S 2019 Rheumatoid arthritis: atherosclerosis imaging and cardiovascular risk assessment using machine and deep learning–based tissue characterization *Curr. Atheroscler. Rep.* **21** 7
[30] Jamthikar A, Gupta D, Khanna N N, Araki T, Saba L, Nicolaides A, Sharma A, Omerzu T, Suri H S and Gupta A 2019 A special report on changing trends in preventive stroke/cardiovascular risk assessment via B-mode ultrasonography *Curr. Atheroscler Rep.* **21** 25
[31] Schnee J M and Hsueh W A 2000 Angiotensin II, adhesion, and cardiac fibrosis *Cardiovasc. Res.* **46** 264–8
[32] Wu L L, Yang N, Roe C J, Cooper M E, Gilbert R E, Atkins R C and Lan H Y 1997 Macrophage and myofibroblast proliferation in remnant kidney: role of angiotensin II *Kidney Int. Suppl.* **63** S221–5
[33] Sun Y, Ramires F J and Weber K T 1997 Fibrosis of atria and great vessels in response to angiotensin II or aldosterone infusion *Cardiovasc. Res.* **35** 138–47

[34] Morihara K, Takai S, Takenaka H, Sakaguchi M, Okamoto Y, Morihara T, Miyazaki M and Kishimoto S 2006 Cutaneous tissue angiotensin–converting enzyme may participate in pathologic scar formation in human skin *J. Am. Acad. Dermatol.* **54** 251–7
[35] Cosyns B, Lochy S, Luchian M L, Gimelli A, Pontone G, Allard S D, de Mey J, Rosseel P, Dweck M and Petersen S E 2020 The role of cardiovascular imaging for myocardial injury in hospitalized COVID-19 patients *Eur. Heart J. Cardiovasc. Imaging* **21** 709–14
[36] Inciardi R M, Lupi L, Zaccone G, Italia L, Raffo M, Tomasoni D, Cani D S, Cerini M, Farina D and Gavazzi E 2020 Cardiac involvement in a patient with coronavirus disease 2019 (COVID-19) *JAMA Cardiol* **5** 819–24
[37] Kim I-C, Kim J Y, Kim H A and Han S 2020 COVID-19-related myocarditis in a 21-year-old female patient *Eur. Heart J.* **41** 1859–9
[38] Kiamanesh O, Harper L, Wiskar K, Luksun W, McDonald M, Ross H, Woo A and Granton J 2020 Lung ultrasound for cardiologists in the time of COVID-19 *Can. J. Cardiol* **36** 1144–7
[39] Zieleskiewicz L, Duclos G, Dransart-Rayé O, Nowobilski N and Bouhemad B 2020 Ultrasound findings in patients with COVID-19 pneumonia in early and late stages: two case-reports *Anaesth. Crit. Care Pain Med* **39** 571–3
[40] Saba L, Tiwari A, Biswas M, Gupta S K, Godia-Cuadrado E, Chaturvedi A, Turk M, Suri H S, Orru S and Sanches J M 2019 Wilson's disease: a new perspective review on its genetics, diagnosis and treatment *Front. Biosci. (Elite edition)* **11** 166–85
[41] Collaborators NASCET 1991 Beneficial effect of carotid endarterectomy in symptomatic patients with high-grade carotid stenosis *New Engl. J. Med.* **325** 445–53
[42] Sanches J M, Laine A F and Suri J S 2012 *Ultrasound Imaging* (Berlin: Springer)
[43] Suri J S, Wilson D and Laxminarayan S 2005 *Handbook of Biomedical Image Analysis* vol 2 43 (New York: Springer Science & Business Media)
[44] Suri J S and Laxminarayan S 2003 *Angiography and Plaque Imaging: Advanced Segmentation Techniques* (Boca Raton, FL: CRC Press)
[45] Acharya U R, Mookiah M R K, Sree S V, Afonso D, Sanches J, Shafique S, Nicolaides A and Pedro L M 2013 Atherosclerotic plaque tissue characterization in 2D ultrasound longitudinal carotid scans for automated classification: a paradigm for stroke risk assessment *Med. Biol. Eng. Comput.* **51** 513–23
[46] Acharya U R, Faust O, Sree S V, Alvin A P C, Krishnamurthi G, Sanches J and Suri J S 2011 Atheromatic™: symptomatic vs. asymptomatic classification of carotid ultrasound plaque using a combination of HOS, DWT & texture *2011 Annual Int. Conf. of the IEEE Engineering in Medicine and Biology Society* (Piscataway, NJ: IEEE) pp 4489–92
[47] Acharya U R, Sree S V, Kulshreshtha S, Molinari F, Koh J E W, Saba L and Suri J S 2014 GyneScan: an improved online paradigm for screening of ovarian cancer via tissue characterization *Technol. Cancer Res. Treat.* **13** 529–39
[48] Biswas M, Kuppili V, Edla D R, Suri H S, Saba L, Marinhoe R T, Sanches J M and Suri J S 2018 Symtosis: a liver ultrasound tissue characterization and risk stratification in optimized deep learning paradigm *Comput. Methods Prog. Biomed.* **155** 165–77
[49] Acharya U R, Krishnan M M R, Sree S V, Sanches J, Shafique S, Nicolaides A, Pedro L M and Suri J S 2012 Plaque tissue characterization and classification in ultrasound carotid scans: a paradigm for vascular feature amalgamation *IEEE Trans. Instrum. Meas.* **62** 392–400
[50] Molinari F, Liboni W, Pavanelli E, Giustetto P, Badalamenti S and Suri J S 2007 Accurate and automatic carotid plaque characterization in contrast enhanced 2-D ultrasound images

*2007 29th Annual Int. Conf. of the IEEE Engineering in Medicine and Biology Society* (Piscataway, NJ: IEEE) pp 335–8

[51] Acharya U, Vinitha Sree S, Mookiah M, Yantri R, Molinari F, Zieleźnik W, Małyszek-Tumidajewicz J, Stępień B, Bardales R and Witkowska A 2013 Diagnosis of Hashimoto's thyroiditis in ultrasound using tissue characterization and pixel classification *Proc. Inst. Mech. Eng. Part H J. Eng. Med.* **227** 788–98

[52] Sharma A M, Gupta A, Kumar P K, Rajan J, Saba L, Nobutaka I, Laird J R, Nicolades A and Suri J S 2015 A review on carotid ultrasound atherosclerotic tissue characterization and stroke risk stratification in machine learning framework *Curr. Atheroscler. Rep.* **17** 55

[53] Ravì D, Wong C, Deligianni F, Berthelot M, Andreu-Perez J, Lo B and Yang G-Z 2016 Deep learning for health informatics *IEEE J. Biomed. Health Inform.* **21** 4–21

[54] Saba L, Biswas M, Kuppili V, Godia E C, Suri H S, Edla D R, Omerzu T, Laird J R, Khanna N N and Mavrogeni S 2019 The present and future of deep learning in radiology *Eur. J. Radiol* **114** 14–24

[55] Biswas M, Kuppili V, Saba L, Edla D R, Suri H S, Cuadrado-Godia E, Laird J, Marinhoe R, Sanches J and Nicolaides A 2019 State-of-the-art review on deep learning in medical imaging *Front. Biosci. (Landmark Ed)* **24** 392–426

[56] Biswas M, Kuppili V, Araki T, Edla D R, Godia E C, Saba L, Suri H S, Omerzu T, Laird J R and Khanna N N 2018 Deep learning strategy for accurate carotid intima-media thickness measurement: an ultrasound study on Japanese diabetic cohort *Comput. Biol. Med.* **98** 100–17

[57] Jamthikar A, Gupta D, Khanna N N, Saba L, Araki T, Viskovic K, Suri H S, Gupta A, Mavrogeni S and Turk M 2019 A low-cost machine learning-based cardiovascular/stroke risk assessment system: integration of conventional factors with image phenotypes *Cardiovasc. Diagn. Ther.* **9** 420

[58] Hoffmann M, Kleine-Weber H, Schroeder S, Krüger N, Herrler T, Erichsen S, Schiergens T S, Herrler G, Wu N-H and Nitsche A 2020 SARS-CoV-2 cell entry depends on ACE2 and TMPRSS2 and is blocked by a clinically proven protease inhibitor *Cell* **181** 271–80

[59] de Wit E, van Doremalen N, Falzarano D and Munster V J 2016 SARS and MERS: recent insights into emerging coronaviruses *Nat. Rev. Microbiol.* **14** 523

[60] Wu K, Peng G, Wilken M, Geraghty R J and Li F 2012 Mechanisms of host receptor adaptation by severe acute respiratory syndrome coronavirus *J. Biol. Chem.* **287** 8904–11

[61] Patel V B, Zhong J-C, Grant M B and Oudit G Y 2016 Role of the ACE2/angiotensin 1–7 axis of the renin–angiotensin system in heart failure *Circ. Res.* **118** 1313–26

[62] Zou X, Chen K, Zou J, Han P, Hao J and Han Z 2020 Single-cell RNA-seq data analysis on the receptor ACE2 expression reveals the potential risk of different human organs vulnerable to 2019-nCoV infection *Front. Med.* **14** 185–192

[63] Hamming I, Timens W, Bulthuis M, Lely A, Navis G and van Goor H 2004 Tissue distribution of ACE2 protein, the functional receptor for SARS coronavirus. A first step in understanding SARS pathogenesis *J. Pathol.* **203** 631–7

[64] Giacomelli A, Pezzati L, Conti F, Bernacchia D, Siano M, Oreni L, Rusconi S, Gervasoni C, Ridolfo A L and Rizzardini G 2020 Self-reported olfactory and taste disorders in patients with severe acute respiratory coronavirus 2 infection: a cross-sectional study *Clin. Infect Dis.* **71** 889–90

[65] Wu A, Peng Y, Huang B, Ding X, Wang X, Niu P, Meng J, Zhu Z, Zhang Z and Wang J 2020 Genome composition and divergence of the novel coronavirus (2019-nCoV) originating in China *Cell Host Microbe* **27** 325–8
[66] Koyuncu O O, Hogue I B and Enquist L W 2013 Virus infections in the nervous system *Cell Host Microbe* **13** 379–93
[67] Desforges M, Le Coupanec A, Dubeau P, Bourgouin A, Lajoie L, Dubé M and Talbot P J 2020 Human coronaviruses and other respiratory viruses: underestimated opportunistic pathogens of the central nervous system? *Viruses* **12** 14
[68] McCray P B, Pewe L, Wohlford-Lenane C, Hickey M, Manzel L, Shi L, Netland J, Jia H P, Halabi C and Sigmund C D 2007 Lethal infection of K18-hACE2 mice infected with severe acute respiratory syndrome coronavirus *J. Virol.* **81** 813–21
[69] Li K, Wohlford-Lenane C, Perlman S, Zhao J, Jewell A K, Reznikov L R, Gibson-Corley K N, Meyerholz D K and McCray P B 2016 Middle East respiratory syndrome coronavirus causes multiple organ damage and lethal disease in mice transgenic for human dipeptidyl peptidase 4 *J. Infect. Dis.* **213** 712–22
[70] Netland J, Meyerholz D K, Moore S, Cassell M and Perlman S 2008 Severe acute respiratory syndrome coronavirus infection causes neuronal death in the absence of encephalitis in mice transgenic for human ACE2 *J. Virol.* **82** 7264–75
[71] Baig A M 2020 Neurological manifestations in COVID-19 caused by SARS-CoV-2 *CNS Neurosci. Ther.* **26** 499
[72] Ryan W 2020 There's a new symptom of coronavirus, doctors say: sudden loss of smell or taste
[73] Hopkins C and Kumar N 2020 Loss of sense of smell as marker of COVID-19 infection *ENT UK* **26** 2020 (https://www.entuk.org/sites/default/files/files/Loss_of_sense_of_smell_as_marker_of_COVID.pdf)
[74] Bohmwald K, Galvez N, Ríos M and Kalergis A M 2018 Neurologic alterations due to respiratory virus infections *Front. Cell. Neurosci.* **12** 386
[75] Zhang H and Baker A 2017 *Recombinant Human ACE2: Acing Out Angiotensin II in ARDS Therapy* (Berlin: Springer)
[76] Radermacher P, Maggiore S M and Mercat A 2017 Fifty years of research in ARDS. Gas exchange in acute respiratory distress syndrome *Am. J. Respir. Crit. Care Med.* **196** 964–84
[77] Chen N, Zhou M, Dong X, Qu J, Gong F, Han Y, Qiu Y, Wang J, Liu Y and Wei Y 2020 Epidemiological and clinical characteristics of 99 cases of 2019 novel coronavirus pneumonia in Wuhan, China: a descriptive study *Lancet* **395** 507–13
[78] Xiong T-Y, Redwood S, Prendergast B and Chen M 2020 Coronaviruses and the cardiovascular system: acute and long-term implications *Eur. Heart J.* **41** 1798–800
[79] Oudit G, Kassiri Z, Jiang C, Liu P, Poutanen S, Penninger J and Butany J 2009 SARS-coronavirus modulation of myocardial ACE2 expression and inflammation in patients with SARS *Eur. J. Clin. Investig.* **39** 618–25
[80] Abdennour L, Zeghal C, Deme M and Puybasset L 2012 Interaction brain-lungs *Ann. Fr. Anesth. Reanim.* e101–7
[81] Fountain J H and Lappin S L 2019 Physiology, Renin Angiotensin System *StatPearls* pp 81 (St Petersburg, FL: StatPearls Publishing)
[82] Rajendran P, Rengarajan T, Thangavel J, Nishigaki Y, Sakthisekaran D, Sethi G and Nishigaki I 2013 The vascular endothelium and human diseases *Int. J. Biol. Sci.* **9** 1057

[83] Lillie P J, Samson A, Li A, Adams K, Capstick R, Barlow G D, Easom N, Hamilton E, Moss P J and Evans A 2020 Novel coronavirus disease (Covid-19): the first two patients in the UK with person to person transmission *J. Infect.* **80** 578–606

[84] Bai Y, Yao L, Wei T, Tian F, Jin D-Y, Chen L and Wang M 2020 Presumed asymptomatic carrier transmission of COVID-19 *JAMA* **323** 1406–7

[85] Mehta P, McAuley D F, Brown M, Sanchez E, Tattersall R S and Manson J J 2020 COVID-19: consider cytokine storm syndromes and immunosuppression *Lancet* **395** 1033–4

[86] Siddiqi H K and Mehra M R 2020 COVID-19 illness in native and immunosuppressed states: a clinical-therapeutic staging proposal *J. Heart Lung Transp.* **39** 405–7

[87] Yin C, Wang C, Tang Z, Wen Y, Zhang S and Wang B 2004 Clinical analysis of multiple organ dysfunction syndrome in patients suffering from SARS *Zhongguo wei zhong bing ji jiu yi xue= Chin. Crit. Care Med.= Zhongguo weizhongbing jijiuyixue* **16** 646–50

[88] Schoenhagen P, Tuzcu E M and Ellis S G 2002 Plaque vulnerability, plaque rupture, and acute coronary syndromes: (multi)-focal manifestation of a systemic disease process *Circulation*

[89] Tisoncik J R, Korth M J, Simmons C P, Farrar J, Martin T R and Katze M G 2012 Into the eye of the cytokine storm *Microbiol. Mol. Biol. Rev.* **76** 16–32

[90] Tersalvi G, Vicenzi M, Calabretta D, Biasco L, Pedrazzini G and Winterton D 2020 Elevated troponin in patients with Coronavirus Disease 2019 (COVID-19): possible mechanisms *J. Cardiac Failure* **26** 470–75

[91] Gomes V A 2020 COVID-19 Cardiac repercussions *Rev. Bras. Fisiol. Exer.* **19**

[92] Zeng J H, Liu Y-X, Yuan J, Wang F-X, Wu W-B, Li J-X, Wang L-F, Gao H, Wang Y and Dong C-F 2020 *First Case of COVID-19 Infection with Fulminant Myocarditis Complication: Case Report and Insights*

[93] Cieszanowski A, Czekajska E, Giżycka B, Gruszczyńska K, Podgórska J, Oronowicz-Jaśkowiak A, Serafin Z, Szurowska E and Walecki J M 2020 Management of patients with COVID-19 in radiology departments, and indications regarding imaging studies–recommendations of the Polish Medical Society of Radiology *Pol. J. Radiol.* **85** e209

[94] Kim D J, Jelic T, Woo M Y, Heslop C and Olszynski P 2020 Just the facts: recommendations on point of care ultrasound use and machine infection control during the COVID-19 pandemic *Can. J. Emerg. Med.* **22** 1–7

[95] An X, Song Z, Gao Y, Tao J and Yang J 2020 To resume noninvasive imaging detection safely after peak period of COVID-19: experiences from Wuhan China *Dermatol. Ther.* **33** e13590

[96] Jakhar D, Kaur I and Kaul S 2020 Art of performing dermoscopy during the times of coronavirus disease (COVID-19): simple change in approach can save the day! *J. Eur. Acad. Dermatol. Venereol.*

[97] Skulstad H, Cosyns B, Popescu B A, Galderisi M, Salvo G D, Donal E, Petersen S, Gimelli A, Haugaa K H and Muraru D 2020 COVID-19 pandemic and cardiac imaging: EACVI recommendations on precautions, indications, prioritization, and protection for patients and healthcare personnel *Eur. Heart J.-Cardiovasc. Imaging* **21** 592–98

[98] Lo S, Yong A, Sinhal A, Shetty S, McCann A, Clark D, Galligan L, El-Jack S, Sader M and Tan R 2020 Consensus guidelines for interventional cardiology services delivery during COVID-19 pandemic in Australia and New Zealand *Heart Lung Circ* **29** 69–77

[99] El-Baz A, Jiang X and Suri J S 2016 *Biomedical Image Segmentation: Advances and Trends* (Boca Raton, FL: CRC Press)

[100] El-Baz A S, Acharya R, Mirmehdi M and Suri J S 2011 *Multi Modality State-of-the-Art Medical Image Segmentation and Registration Methodologies* vol 1 (New York: Springer Science & Business Media)
[101] Olusanya O 2020 Ultrasound in times of COVID-19 *ICU Management & Practice* **20** 43–50
[102] Smith M, Hayward S, Innes S and Miller A 2020 Point-of-care lung ultrasound in patients with COVID-19: a narrative review *Anaesthesia* **75** 1096–104
[103] Jacobi A, Chung M, Bernheim A and Eber C 2020 Portable chest X-ray in coronavirus disease-19 (COVID-19): a pictorial review *Clin. Imaging* **64** 35–42
[104] Chung M, Bernheim A, Mei X, Zhang N, Huang M, Zeng X, Cui J, Xu W, Yang Y and Fayad Z A 2020 CT imaging features of 2019 novel coronavirus (2019-nCoV) *Radiology* **295** 202–7
[105] Vasilev Y, Sergunova K, Bazhin A, Masri A, Vasileva Y, Suleumanov E, Semenov D, Kudryavtsev N, Panina O and Khoruzhaya A 2020 MRI of the lungs in patients with COVID-19: clinical case *JMRI* **79** 13–9
[106] Huang L, Zhao P, Tang D, Zhu T, Han R, Zhan C, Liu W, Zeng H, Tao Q and Xia L 2020 Cardiac involvement in recovered COVID-19 patients identified by magnetic resonance imaging *JACC: Cardiovasc. Imaging* **13** 2330–9
[107] Luetkens J A, Isaak A, Zimmer S, Nattermann J, Sprinkart A M, Boesecke C, Rieke G J, Zachoval C, Heine A and Velten M 2020 Diffuse myocardial inflammation in covid-19 associated myocarditis detected by multiparametric cardiac magnetic resonance imaging *Circ.: Cardiovasc. Imaging* **13** e010897
[108] Poyiadji N, Shahin G, Noujaim D, Stone M, Patel S and Griffith B 2020 COVID-19–associated acute hemorrhagic necrotizing encephalopathy: CT and MRI features *Radiology* **296** 201187
[109] Kandemirli S G, Dogan L, Sarikaya Z T, Kara S, Akinci C, Kaya D, Kaya Y, Yildirim D, Tuzuner F and Yildirim M S 2020 Brain MRI findings in patients in the intensive care unit with COVID-19 infection *Radiology* **297** 201697
[110] Bhayana R, Som A, Li M D, Carey D E, Anderson M A, Blake M A, Catalano O, Gee M S, Hahn P F and Harisinghani M 2020 Abdominal imaging findings in COVID-19: preliminary observations *Radiology* **297** 201908
[111] Eliezer M and Hautefort C 2020 MRI evaluation of the olfactory clefts in patients with SARS-CoV-2 infection revealed an unexpected mechanism for olfactory function loss *Acad. Radiol.* **27** 1191
[112] Xiao Z, Xu C, Wang D and Zeng H 2020 The experience of treating patients with acute myocardial infarction under the COVID-19 epidemic *Catheter. Cardiovasc. Interv.* **97** E244–8
[113] Meyer P, Degrauwe S, Van Delden C, Ghadri J-R and Templin C 2020 Typical takotsubo syndrome triggered by SARS-CoV-2 infection *Eur. Heart J.* **41** 1860–0
[114] Danzi G B, Loffi M, Galeazzi G and Gherbesi E 2020 Acute pulmonary embolism and COVID-19 pneumonia: a random association? *Eur. Heart J.* **41** 1858–8
[115] Zhang L, Feng X, Zhang D, Jiang C, Mei H, Wang J, Zhang C, Li H, Xia X and Kong S 2020 Deep vein thrombosis in hospitalized patients with coronavirus disease 2019 (COVID-19) in Wuhan, China: prevalence, risk factors, and outcome *Circulation* **142** 114–28
[116] Emanuel E J, Persad G, Upshur R, Thome B, Parker M, Glickman A, Zhang C, Boyle C, Smith M and Phillips J P 2020 Fair Allocation of Scarce Medical Resources in the Time of Covid-19 *N Engl. J. Med.* **382** 2049–55

[117] Rosenbaum L 2020 Facing Covid-19 in Italy—ethics, logistics, and therapeutics on the epidemic's front line *New Engl. J. Med.* **382** 1873–5
[118] Bhatt A S *et al* 2020 Declines in hospitalizations for acute cardiovascular conditions during the COVID-19 pandemic: a multicenter tertiary care experience *J. Am. Coll. Cardiol.* **76** 280–8
[119] Vaishya R, Haleem A, Vaish A and Javaid M 2020 Emerging technologies to combat COVID-19 pandemic *J. Clin. Exp. Hepatol* **10** 409–11
[120] Murphy K, Smits H, Knoops A J, Korst M B, Samson T, Scholten E T, Schalekamp S, Schaefer-Prokop C M, Philipsen R H and Meijers A 2020 COVID-19 on the chest radiograph: a multi-reader evaluation of an AI system *Radiology* **296** 201874
[121] Zheng N, Du S, Wang J, Zhang H, Cui W, Kang Z, Yang T, Lou B, Chi Y and Long H 2020 Predicting COVID-19 in China using hybrid AI model *IEEE Trans. Cybern* **50** 2891–904
[122] Chieffo A, Stefanini G G, Price S, Barbato E, Tarantini G, Karam N, Moreno R, Buchanan G L, Gilard M and Halvorsen S 2020 EAPCI position statement on invasive management of acute coronary syndromes during the COVID-19 pandemic *Eur. Heart J.* **41** 1839–51
[123] Salehi S, Abedi A, Balakrishnan S and Gholamrezanezhad A 2020 Coronavirus disease 2019 (COVID-19): a systematic review of imaging findings in 919 patients *Am. J. Roentgenol.* **215** 1–7
[124] Dangis A, Gieraerts C, Bruecker Y D, Janssen L, Valgaeren H, Obbels D, Gillis M, Ranst M V, Frans J and Demeyere A 2020 Accuracy and reproducibility of low-dose submillisievert chest CT for the diagnosis of COVID-19 *Radiol.: Cardiothorac. Imaging* **2** e200196
[125] Rubin G D, Ryerson C J, Haramati L B, Sverzellati N, Kanne J P, Raoof S, Schluger N W, Volpi A, Yim J-J and Martin I B 2020 The role of chest imaging in patient management during the COVID-19 pandemic: a multinational consensus statement from the Fleischner Society *Chest* **158** 106–16
[126] Nair A *et al* 2020 Society of Thoracic Imaging statement: considerations in designing local imaging diagnostic algorithms for the COVID-19 pandemic *Clin. Radiol.* **75** 329–34
[127] Laghi A 2020 Cautions about radiologic diagnosis of COVID-19 infection driven by artificial intelligence *Lancet Digit. Health* **2** e225
[128] Miotto R, Wang F, Wang S, Jiang X and Dudley J T 2018 Deep learning for healthcare: review, opportunities and challenges *Brief. Bioinform.* **19** 1236–46
[129] Esteva A, Robicquet A, Ramsundar B, Kuleshov V, DePristo M, Chou K, Cui C, Corrado G, Thrun S and Dean J 2019 A guide to deep learning in healthcare *Nat. Med.* **25** 24–9
[130] Hosny A, Parmar C, Quackenbush J, Schwartz L H and Aerts H J 2018 Artificial intelligence in radiology *Nat. Rev. Cancer* **18** 500–10
[131] Sinha JSS G R 2019 *Cognitive Informatics, Computer Modelling, and Cognitive Science: Volume 1: Theory, Case Studies, and Applications* (Netherlands: Elsevier)
[132] Tang X 2019 The role of artificial intelligence in medical imaging research *BJR| Open* **2** 20190031
[133] Saeian K, Rhyne T L and Sagar K B 1994 Ultrasonic tissue characterization for diagnosis of acute myocardial infarction in the coronary care unit *Am. J. Cardiol.* **74** 1211–5
[134] Mavrogeni S, Sfikakis P P, Gialafos E, Bratis K, Karabela G, Stavropoulos E, Spiliotis G, Sfendouraki E, Panopoulos S and Bournia V 2014 Cardiac tissue characterization and the

diagnostic value of cardiovascular magnetic resonance in systemic connective tissue diseases *Arthritis Care Res.* **66** 104–12

[135] Wu J, Pan J, Teng D, Xu X, Feng J and Chen Y-C 2020 Interpretation of CT signs of 2019 novel coronavirus (COVID-19) pneumonia *Eur. Radiol.* **30** 5455–62

[136] Alimadadi A, Aryal S, Manandhar I, Munroe P B, Joe B and Cheng X 2020 Artificial Intelligence and Machine Learning to Fight COVID-19 *Physiological Genomics* **52** 200–2

[137] Vaishya R, Javaid M, Khan I H and Haleem A 2020 Artificial intelligence (AI) applications for COVID-19 pandemic *Diabetes Metab. Syndr.: Clin. Res. Rev.* **14** 337–9

[138] Jamthikar A, Gupta D, Saba L, Khanna N N, Araki T, Viskovic K, Mavrogeni S, Laird J R, Pareek G and Miner M *et al* 2020 Cardiovascular/stroke risk predictive calculators: a comparison between statistical and machine learning models *Cardiovasc. Diagn. Ther* **10** 919–38

[139] Jamthikar A, Gupta D, Khanna N N, Saba L, Laird J R and Suri J S 2020 Cardiovascular/stroke risk prevention: a new machine learning framework integrating carotid ultrasound image-based phenotypes and its harmonics with conventional risk factors *Indian Heart J.* **72** 258–64

[140] Biswas M, Kuppili V, Edla D R, Suri H S, Saba L, Marinhoe R T, Sanches J M and Suri J S 2017 Symtosis: a liver ultrasound tissue characterization and risk stratification in optimized deep learning paradigm *Comput. Methods Prog. Biomed* **155** 165–77

[141] Bishop C M 2006 *Pattern Recognition and Machine Learning* (New York: Springer)

[142] LeCun Y, Bengio Y and Hinton G 2015 Deep learning *Nature* **521** 436–44

[143] Suri J S, Acharya U R, Faust O, Alvin A P C, Sree S V, Molinari F, Saba L and Nicolaides A 2011 Symptomatic vs. asymptomatic plaque classification in carotid ultrasound *J. Med. Syst.* **36** 1861–71

[144] Cortes C and Vapnik V 1995 Support-vector networks *Mach. Learn.* **20** 273–97

[145] Mirmehdi M 2008 *Handbook of Texture Analysis* (Singapore: Imperial College Press)

[146] Bharati M H, Liu J J and MacGregor J F 2004 Image texture analysis: methods and comparisons *Chemometr. Intell. Lab. Syst.* **72** 57–71

[147] Acharya U R, Chua C K, Lim T-C, Dorithy T and Suri J S 2009 Automatic identification of epileptic EEG signals using nonlinear parameters *J. Mech. Med. Biol.* **9** 539–53

[148] Acharya U R, Faust O, Sree S V, Molinari F and Suri J S 2012 ThyroScreen system: high resolution ultrasound thyroid image characterization into benign and malignant classes using novel combination of texture and discrete wavelet transform *Comput. Methods Programs Biomed.* **107** 233–41

[149] Reynolds D A 2009 Gaussian mixture models *Encyclopedia of Biometrics* (Berlin: Springer) 741

[150] Huang D-S 1999 Radial basis probabilistic neural networks: model and application *Int. J. Pattern Recognit Artif Intell.* **13** 1083–101

[151] Quinlan J R 1987 Generating production rules from decision trees *IJCAI* **87** 304–7

[152] Clark P J and Evans F C 1954 Distance to nearest neighbor as a measure of spatial relationships in populations *Ecology* **35** 445–53

[153] Rish I 2001 An empirical study of the naive Bayes classifier *IJCAI 2001 Workshop on Empirical Methods in Artificial Intelligence* pp 41–6

[154] Ross T J 2009 *Fuzzy Logic with Engineering Applications* (University of New Mexico: Wiley)

[155] Kadyrov A and Petrou M 2001 The trace transform and its applications *IEEE Trans. Pattern Anal. Mach. Intell.* **23** 811–28
[156] Jawahar C and Ray A 1996 Incorporation of gray-level imprecision in representation and processing of digital images *Pattern Recognit. Lett.* **17** 541–6
[157] Galloway M M 1974 Texture analysis using grey level run lengths *STIN* **75** 18555
[158] Boi A, Jamthikar A D, Saba L, Gupta D, Sharma A, Loi B, Laird J R, Khanna N N and Suri J S 2018 A survey on coronary atherosclerotic plaque tissue characterization in intravascular optical coherence tomography *Curr. Atheroscler. Rep.* **20** 33
[159] Jamthikar A, Gupta D, Khanna N N, Saba L, Araki T, Viskovic K, Suri H S, Gupta A, Mavrogeni S and Turk M *et al* 2019 A low-cost machine learning-based cardiovascular/stroke risk assessment system: integration of conventional factors with image phenotypes *Cardiovasc. Diagn. Ther.* **9** 420
[160] Jamthikar A, Gupta D, Khanna N N, Araki T, Saba L, Nicolaides A, Sharma A, Omerzu T, Suri H S and Gupta A *et al* 2019 A special report on changing trends in preventive stroke/cardiovascular risk assessment via B-Mode ultrasonography *Curr. Atheroscler. Rep.* 21 25
[161] Viswanathan V *et al* 2020 Does the carotid bulb offer a better 10-Year CVD/stroke risk assessment compared to the common carotid artery? A 1516 ultrasound scan study *Angiology* **71** 3319720941730
[162] Long J, Shelhamer E and Darrell T 2015 Fully convolutional networks for semantic segmentation *Proc. of the IEEE Conf. on Computer Vision and Pattern Recognition* pp 3431–40
[163] Biswas M, Kuppili V, Saba L, Edla D R, Suri H S, Sharma A, Cuadrado-Godia E, Laird J R, Nicolaides A and Suri J S 2019 Deep learning fully convolution network for lumen characterization in diabetic patients using carotid ultrasound: a tool for stroke risk *Med. Biol. Eng. Comput.* **57** 543–64
[164] Saba L, Biswas M, Suri H S, Viskovic K, Laird J R, Cuadrado-Godia E, Nicolaides A, Khanna N, Viswanathan V and Suri J S 2019 Ultrasound-based carotid stenosis measurement and risk stratification in diabetic cohort: a deep learning paradigm *Cardiovasc. Diagn. Ther.* **9** 439
[165] Dong D, Tang Z, Wang S, Hui H, Gong L, Lu Y, Xue Z, Liao H, Chen F and Yang F 2020 The role of imaging in the detection and management of COVID-19: a review *IEEE Rev. Biomed. Eng*
[166] Ito R I S and Naganawa S 2020 A review on the use of artificial intelligence for medical imaging of the lungs of patients with coronavirus disease 2019 *Diagn. Interv. Radiol*
[167] Lu W, Zhang S, Chen B, Chen J, Xian J, Lin Y, Shan H and Su Z Z 2020 A clinical study of noninvasive assessment of lung lesions in patients with coronavirus disease-19 (COVID-19) by bedside ultrasound *Ultraschall in der Medizin-Eur. J. Ultrasound* **41** 300–7
[168] Kang H, Xia L, Yan F, Wan Z, Shi F, Yuan H, Jiang H, Wu D, Sui H and Zhang C 2020 Diagnosis of coronavirus disease 2019 (covid-19) with structured latent multi-view representation learning *IEEE Trans. Med. Imaging* **39** 2606–14
[169] Xinggang Wang X D, Fu Q, Zhou Q, Zhou Q, Feng J, Ma H, Liu W and Zheng C 2020 A weakly-supervised framework for COVID-19 classification and lesion localization from chest CT *IEEE Trans. Med. Imaging* **39** 2615–25
[170] Krizhevsky A, Sutskever I and Hinton G E 2012 *Imagenet classification with deep convolutional neural networks Advances in Neural Information Processing Systems 25 (NIPS 2012)* F. Pereira *et al* (Cambridge, MA: MIT Press) 1097–105

[171] Szegedy C, Vanhoucke V, Ioffe S, Shlens J and Wojna Z 2016 Rethinking the inception architecture for computer vision *Proc. of the IEEE Conf. on Computer Vision and Pattern Recognition* pp 2818–26
[172] Wang K, Lu X, Zhou H, Gao Y, Zheng J, Tong M, Wu C, Liu C and Huang L 2019 Deep learning Radiomics of shear wave elastography significantly improved diagnostic performance for assessing liver fibrosis in chronic hepatitis B: a prospective multicentre study *Gut* **68** 729–41
[173] Wang S *et al* 2020 A fully automatic deep learning system for COVID-19 diagnostic and prognostic analysis *Eur. Respir. J.* **56** 2000775
[174] Zhang K *et al* 2020 Clinically applicable AI system for accurate diagnosis, quantitative measurements, and prognosis *Cell* **182** 1360
[175] Li Z *et al* 2020 from community acquired pneumonia to COVID-19: a deep learning based method for quantitative analysis of COVID-19 on thick-section CT scans *Medrxiv* 2020
[176] Chen J *et al* 2020 Deep learning-based model for detecting 2019 novel coronavirus pneumonia on high-resolution computed tomography: a prospective study *Sci. Rep.* **10** 19196
[177] Angel C T (http://121.40.75.149/znyx-ncov/index#/app/index) (accessed 24 July 2020)
[178] Yang S, Jiang L, Cao Z, Wang L, Cao J, Feng R, Zhang Z, Xue X, Shi Y and Shan F 2020 Deep learning for detecting corona virus disease 2019 (COVID-19) on high-resolution computed tomography: a pilot study *Ann. Transl. Med.* **8**
[179] Oh Y, Park S and Ye J C 2020 Deep learning Covid-19 features on CXR using limited training data sets *IEEE Trans. Med. Imaging* **39** 2688–700
[180] Ren Z H, Mu W C and Huang S Y 2018 Design and optimization of a ring-pair permanent magnet array for head imaging in a low-field portable MRI system *IEEE Trans. Magn.* **55** 1–8
[181] Cooley C Z, Stockmann J P, Armstrong B D, Sarracanie M, Lev M H, Rosen M S and Wald L L 2015 Two-dimensional imaging in a lightweight portable MRI scanner without gradient coils *Magn. Reson. Med.* **73** 872–83
[182] Mirvis S E 1999 Use of portable CT in the R Adams Cowley Shock Trauma Center: experiences in the admitting area, ICU, and operating room *Surg. Clin. North Am.* **79** 1317–30
[183] Wang X and Bhatt D L 2020 COVID-19: an unintended force for medical revolution *J. Invasive Cardiol.* **32** E81–2
[184] Thamman R, Gulati M, Narang A, Utengen A, Mamas M A and Bhatt D L 2020 Twitter-based learning for continuing medical education? *Eur. Heart J.*
[185] Li L, Zhang Q, Wang X, Zhang J, Wang T, Gao T-L, Duan W, Tsoi K K-F and Wang F-Y 2020 Characterizing the propagation of situational information in social media during COVID-19 epidemic: a case study on weibo *IEEE Trans. Comput. Soc. Syst.* **7** 556–62
[186] El-Baz A and Suri J S (ed) 2019 *Big Data in Multimodal Medical Imaging* (Boca Raton, FL: CRC Press)
[187] Kooraki S, Hosseiny M, Myers L and Gholamrezanezhad A 2020 Coronavirus (COVID-19) outbreak: what the department of radiology should know *J. Am. Coll. Radiol* **17** 447–51
[188] Mossa-Basha M, Medverd J, Linnau K, Lynch J B, Wener M H, Kicska G, Staiger T and Sahani D 2020 Policies and guidelines for COVID-19 preparedness: experiences from the University of Washington *Radiology* **296** 201326

[189] Buonsenso D, Piano A, Raffaelli F, Bonadia N, Donati K D G and Franceschi F 2020 novel coronavirus disease-19 pnemoniae: a case report and potential applications during COVID-19 outbreak *Eur. Rev. Med. Pharmacol. Sci.* **24** 2776–80

[190] Suri J S *et al* 2020 COVID-19 pathways for brain and heart injury in comorbidity patients: A role of medical imaging and artificial intelligence-based COVID severity classification: A review *Comput. Biol. Med.* **124** 103960